RSC Advances

PAPER

View Article Online
View Journal | View Issue

Cite this: *RSC Adv.*, 2023, **13**, 13586

LZY3016, a novel geldanamycin derivative, inhibits tumor growth in an MDA-MB-231 xenograft model†

Zhenyu Li,[a] Lejiao Jia,[b] Hui Tang,[a] Yuemao Shen[c] and Chengwu Shen *[a]

Received 31st March 2023
Accepted 26th April 2023

DOI: 10.1039/d3ra02131a

rsc.li/rsc-advances

A novel geldanamycin derivative LZY3016 was synthesized as an antitumor agent. Compound LZY3016 exhibited potent anti-proliferation activity toward MDA-MB-231 (IC_{50} = 0.06 μM), which was more effective than positive drug 17-AAG. *In vivo* hepatotoxicity assay displayed that serum AST/ALT levels in LZY3016-treated mice were both significantly less than those in the geldanamycin (GA) group. LZY3016 showed potent antitumor activity in an MDA-MB-231 xenograft mouse model, suggesting LZY3016 is an up-and-coming antitumor candidate. The theoretical binding mode between LZY3016 and Hsp90 was obtained by molecular dynamics simulation.

1. Introduction

Heat shock protein 90 (Hsp90) is a very rich protein in cells, which plays essential regulatory roles by binding to several client proteins. Geldanamycin (GA) was identified as the first natural product inhibitor of Hsp90, which binds to the ATP-binding site of the Hsp90 N-terminal domain, leading to degradation of its client proteins.[1,2] Because of its core role in carcinogenic signal transduction, Hsp90 is an attractive target for cancer treatment.[3]

Although GA has excellent antitumor potentiality, it has not been applied in the clinic due to its poor water solubility, and hepatotoxicity.[4] Subsequently, more stable and soluble GA derivatives were synthesized and promoted to clinical trials,[5,6] such as tanespimycin (17-AAG) and alvespimycin (17-DMAG) (Fig. 1). 17-AAG showed some prospect for the treatment of breast cancer in the phase II clinical trial, however, the clinical trial has been terminated, which indicates that the development of a new generation of GA derivatives with low or even no hepatotoxicity is imminent.

In this study, a novel GA derivative 17-propargylamine-17-demethoxygeldanamycin (LZY3016) was synthesized, because to modify the 17-position of GA with amino substituents could decrease the hepatotoxicity, such as 17-AAG.[7] (Fig. 2). In this paper, the anti-proliferation activity of LZY3016 toward five cancer cells and its *in vivo* hepatotoxicity were determined. In addition, the binding target and antitumor activity in an MDA-MB-231 xenograft model of LZY3016 were also studied.

2. Materials and methods

2.1. General

All melting points were measured on the micro-melting point instrument without correction. ^{1}H NMR spectra and ^{13}C NMR spectra were both obtained by a 600 MHz Bruker Avance spectrometer. API 4000 Mass Spectrometer was used to record the ESI-MS spectra. Thin-layer chromatography (TLC) was carried out on GF254 glass pre-coated silica gel plates. Geldanamycin was purchased from Shanghai Yingrui Chemical Technology Co., Ltd. The AST/ALT Assay Kits were purchased from Shanghai Rongsheng Biological Pharmaceutical Co., Ltd.

2.2. Ethical statement

The experimental animal ethics committee of Shandong Provincial Hospital Affiliated to Shandong First Medical University approved all animal experiments and ensured they are carried out in accordance with the "Guidelines for the Care and Use of Experimental Animals". All efforts are aimed at reducing the number of animals used and the suffering in the experiment.

2.3. Synthesis of LZY3016

Geldanamycin (28 mg, 0.05 mmol) was suspended in 5 mL dichloromethane and then propargylamine (130 μL, 2 mmol) was added, which was stirred at room temperature overnight. After the reaction finished, the mixture was washed with 1.5 N hydrochloric acid solution (2 × 20 mL), followed by brine (3 × 15 mL). The dichloromethane layer was then dehydrated by anhydrous magnesium sulfate, filtered, and evaporated to afford the crude product, which was purified by flash column

[a]*Department of Pharmacy, Shandong Provincial Hospital Affiliated to Shandong First Medical University, Jinan 250021, Shandong, P. R. China. E-mail: scw810@126.com; Fax: +86 531 68778252; Tel: +86 531 68778252*

[b]*Department of Pharmacy, Cheeloo College of Medicine, Shandong University Qilu Hospital, No. 107 West Wenhua Road, Jinan 250012, Shandong, P. R. China*

[c]*Key Laboratory of Chemical Biology (Ministry of Education), School of Pharmaceutical Sciences, Cheeloo College of Medicine, Shandong University, No. 44 West Wenhua Road, Jinan 250012, Shandong, P. R. China*

† Electronic supplementary information (ESI) available. See DOI: https://doi.org/10.1039/d3ra02131a

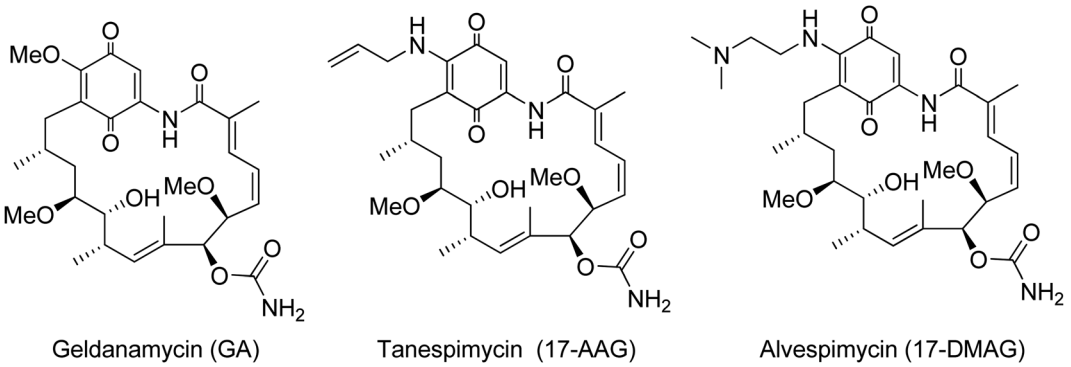

Fig. 1 Known ansamycin Hsp90 inhibitors.

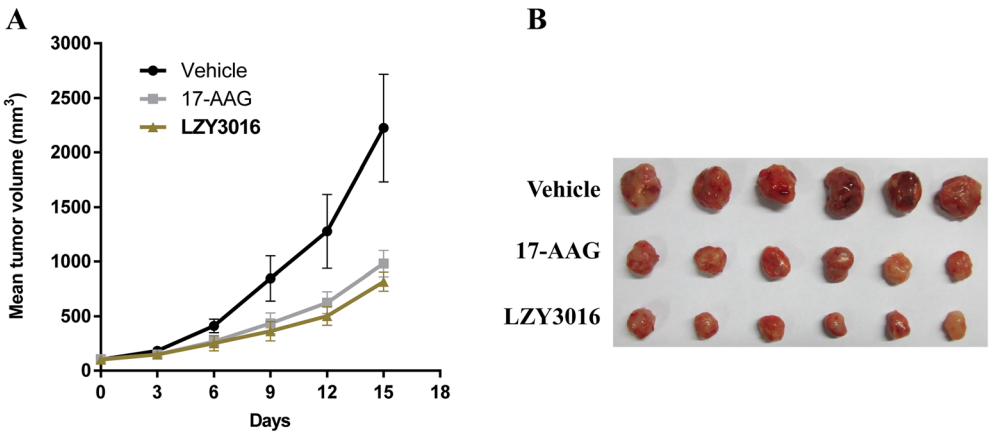

Fig. 2 The tumor growth curve of the MDA-MB-231 xenograft in nude mice (A). Photo of dissected tumor tissues (B).

chromatography on silica gel (petroleum ether/ethyl acetate = 1 : 1) to obtain LZY3016 (28 mg, 95.9%) as a purple solid. M.p. 126–127 °C; ^{1}H NMR (600 MHz, chloroform-d) δ 9.09 (s, 1H), 7.32 (s, 1H), 6.95 (d, J = 11.7 Hz, 1H), 6.59 (t, J = 11.4 Hz, 1H), 6.35 (t, J = 6.0 Hz, 1H), 5.92–5.84 (m, 2H), 5.19 (s, 1H), 4.98 (s, 2H), 4.31 (dt, J = 6.2, 3.3 Hz, 3H), 4.07 (s, 1H), 3.57 (t, J = 7.1 Hz, 1H), 3.47–3.43 (m, 1H), 3.37 (s, 3H), 3.27 (s, 3H), 2.78–2.69 (m, 2H), 2.41 (d, J = 2.5 Hz, 1H), 2.38 (dd, J = 14.3, 10.9 Hz, 1H), 2.04–2.00 (m, 3H), 1.86–1.74 (m, 6H), 1.00 (t, J = 7.6 Hz, 6H); ^{13}C NMR (150 MHz, $CDCl_3$) δ 183.6, 181.6, 168.4, 156.1, 143.9, 140.7, 135.9, 134.9, 133.6, 132.9, 127.0, 126.5, 110.3, 109.1, 81.6, 81.3, 81.1, 78.2, 74.0, 72.6, 57.1, 56.7, 35.4, 34.9, 34.4, 32.3, 28.6, 22.9, 12.8, 12.6, 12.4; ESI-MS: m/z 606.5 $[M + Na]^+$ (calcd 606.7).

2.4. *In vitro* anti-proliferation activity

The cytotoxicities of the compounds against cells were determined by MTT method.[8] The cell inhibitory rate was calculated according to the following equation:

$$\text{Inhibition rate} = \frac{\text{OD control well} - \text{OD treated well}}{\text{OD control well} - \text{OD blank well}} \times 100\%$$

The cytotoxicities of the compounds are showed by IC_{50} value, which is defined as the concentration of the test compounds required to reduce cell viability by 50%.

2.5. *In vivo* hepatotoxicity test

The hepatotoxicity test in mice for the compounds were done according to our previously published study.[8–12] The levels of aspartate aminotransferase (AST) and alanine aminotransferase (ALT) of GA-treated and LZY3016-treated groups were measured using the AST and ALT Assay Kits.

2.6. *In vitro* Hsp90 inhibitory activity

The fluorescence polarization assay (FPA) was done as our previously published papers.[8–12] Briefly, recombinant Hsp90α protein (50 nM), GA-FITC (5 nM), and the tested compounds were added to the reaction mixes (100 μL) in a black 96-well plates, which were recorded on POLARstar® Omega microplate reader (λ_{ex} = 485 nm, λ_{em} = 520 nm) after incubation for 5 h. The IC_{50} is the concentration of the compound replaced 50% bound GA-FITC.

2.7. *In vivo* antitumor activity

Shortly, 5 × 10^6 MDA-MB-231 cells were implanted in the armpit subcutaneous layer of right foreleg of female athymic nude mice (6–7 weeks old). Eighteen mice were divided randomly into LZY3016-treated group, 17-AAG-treated group and vehicle group (six mice in each group) after the average tumor volume reached to 100 mm^3. A dose of 10 mg kg^{-1} actual

body-weight was given intravenously every 3 days. After fifteen days of drug treatment, all the mice were killed and then the tumors were excised and weighted. The tumor growth inhibition (TGI), RTV and relative increment ratio (T/C) were calculated with the following three equations:[13]

$$\mathrm{TGI} = \frac{\text{averaged tumor weight of controlled group} - \text{averaged tumor weight of drug-treated group}}{\text{averaged tumor weight of controlled group}} \quad (1)$$

$$\mathrm{RTV} = \frac{\text{the tumor volume measured at the end of treatment}}{\text{the tumor volume measured at the begining of treatment}} \quad (2)$$

$$\mathrm{T/C} = \frac{\text{mean RTV of drug-treated group}}{\text{mean RTV of control group}} \quad (3)$$

2.8. Molecular docking

We used Autodock Vina 1.1.2 [14] to study the binding pattern between LZY3016 and Hsp90. The Hsp90-GA complex (PDB code: 1YET) was retrieved from RCSB Protein Data Bank.[15,16] AutoDock Tools 1.5.6 package[17,18] was used to prepare PDBQT formats of Hsp90 and LZY3016. The Hsp90 pocket was set as center_x, y, z (40.695, −46.782, 65.693) and size_x, y, z (15, 15, 15). The best pose was chosen for subsequent MD simulation.

2.9. Molecular dynamics simulation

Amber 12 [19–21] was used to optimize the best docking pose. Initially 500 steps of steepest descent minimization followed by 500 steps of conjugate gradient minimization were done. The complex was equilibrated by 100 ps heating and 1000 ps density equilibration with weak restraints. Finally, 40 ns MD simulation was performed using the PMEMD module.

2.10. MM/GBSA calculation and energy decomposition calculation

The equilibrated part of trajectories was used to estimate the binding free energy (ΔG_{bind}) using the MM/GBSA method.[22] To obtain more information with respect to the residues surrounding the binding pocket, the per-residue binding free energy was decomposed into *van der Waals* (ΔE_{vdw}), solvation (ΔE_{sol}), electrostatic (ΔE_{ele}) and total contribution ($\Delta E_{\mathrm{total}}$).

3. Results and discussion

3.1. Preparation of LZY3016

The compound LZY3016 was synthesized by reacting the lead compound GA with the propargylamine as reported in the literature (Scheme 1).[8–11,23,24] The structure of LZY3016 was characterized by ^{1}H-NMR, ^{13}C-NMR and MS spectral data.

3.2. *In vitro* anti-proliferative activity

The antitumor activities of LZY3016 on MDA-MB-231, HepG2, HeLa, A431 and SW480 cancer cell lines were screened by MTT method with 17-AAG and GA as positive controls. *In vitro* cytotoxicities evaluation showed that compound LZY3016 was approximate 8-fold less toxic than the positive control GA toward normal human hepatic cell HL7702 (Table 1). In the cancer cell lines, LZY3016 displayed potent cytotoxicity against MDA-MB-231 cells with an IC_{50} value of 0.06 μM, which was 3.5-fold, 3.1-fold, 12-fold and 3.9-fold more active than that toward HeLa, A431, SW480 and HepG2, respectively, suggesting that

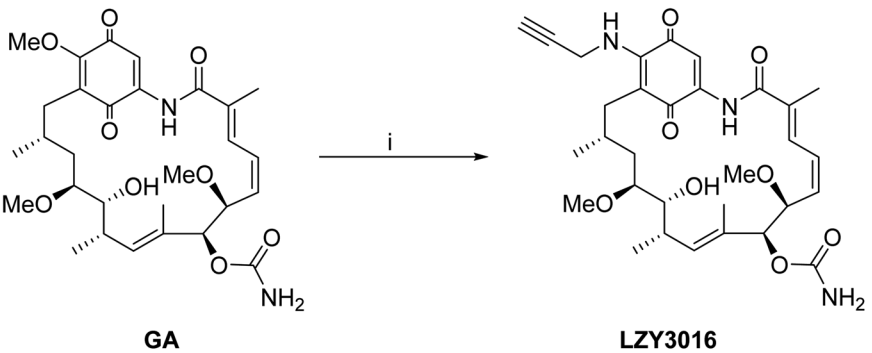

GA LZY3016

Scheme 1 Synthesis route of LZY3016. Reagents and conditions: (i) propargylamine, dichloromethane, room temperature, overnight.

Table 1 *In vitro* cytotoxicities of LZY3016, 17-AAG and GA

	IC_{50} (nM)					
Compd	HL7702	HeLa	MDA-MB-231	A431	SW480	HepG2
LZY3016	1247 ± 263	218 ± 27	60 ± 19	186 ± 47	725 ± 86	236 ± 37
17-AAG	262 ± 35	159 ± 21	338 ± 52	67 ± 5	657 ± 79	86 ± 12
GA	146 ± 15	651 ± 78	65 ± 16	48 ± 9	308 ± 37	41 ± 6

LZY3016 had selective anti-MDA-MB-231 proliferation activity against other four cancer cell lines (Table 1).

3.3. Hepatotoxicity evaluations

In vivo hepatotoxicity test displayed that GA had serious hepatotoxicity due to serum AST/ALT levels of GA-treated mice were significantly increased compared to vehicle group ($P < 0.001$) (Table 2). LZY3016-treated group had significantly lower serum AST level than 17-AAG group ($P < 0.05$), and no significant differences of serum ALT level were found between LZY3016-treated group and 17-AAG-treated group ($P > 0.05$). Interestingly, LZY3016-treated group had significantly lower serum AST/ALT levels than GA group ($P < 0.001$), and no significant differences were found between LZY3016-treated mice and vehicle control mice ($P > 0.05$).

3.4. Hsp90 inhibitory activity

To identify the drug target of LZY3016, using 17-AAG and GA as the positive controls, the Hsp90 binding assay was performed using FPA method to evaluate the inhibitory activity between compound LZY3016 and recombinant Hsp90. It is indicated that Hsp90 inhibitory activity of compound LZY3016 ($IC_{50} = 0.63$ μM) was more active than 17-AAG ($IC_{50} = 0.81$ μM) (Table 3).

3.5. *In vivo* antitumor activity

Inspired with the potent *in vitro* antiproliferative activity of LZY3016 toward MDA-MB-231 cells with no hepatotoxicity, we continue to investigate the antitumor activity *in vivo* in an MDA-MB-231 xenograft model. The antitumor effects were unveiled by tumor weight and volume, which were reflected by calculating the TGI and T/C, respectively. After fifteen days of continuous treatment, compound LZY3016-treated group exhibited higher TGI (60.5%) and lower T/C (38.3%) values than those of 17-AAG-group (TGI = 53.9%, T/C = 43.5%), indicating the excellent *in vivo* antitumor activities of LZY3016 (Table 4). The tumor growth curve and the final tumor tissue size visualized in Fig. 2 explicitly showed the excellent antitumor potency of LZY3016.

Table 2 *In vivo* hepatotoxicity evaluation of LZY3016, GA and vehicle-treated mice

Compd	AST (U L^{-1})	ALT (U L^{-1})
LZY3016	183.3 ± 29.4	75.5 ± 12.8
17-AAG	248.9 ± 21.6	80.2 ± 14.3
GA	358.6 ± 45.2	298.1 ± 31.7
Vehicle	199.5 ± 18.3	65.6 ± 7.2

Table 3 The IC_{50} values of LZY3016, 17-AAG and GA at inhibiting Hsp90α

Compd	IC_{50} (μM)
LZY3016	0.63 ± 0.14
17-AAG	0.81 ± 0.19
GA	0.21 ± 0.08

3.6. Molecular modeling

MD simulation of Hsp90-LZY3016 complex was done using Amber 12 package. The free protein and Hsp90-LZY3016 complex were equilibrated after 40 ns MD simulation, and the plot of RMSDs (in ångstrom) of the two systems were shown in Fig. 3A.

The flexibility of the residues was revealed by calculating the root mean square fluctuations (RMSF) of the whole protein residues in the free protein and Hsp90-LZY3016 complex. The RMSF values of Hsp90 residues in the presence and absence of LZY3016 were clearly exhibited in Fig. 3B. It was showed that most of the residues in the Hsp90 binding site showed minor flexibility with the RMSF less than 2 Å, revealing that these residues seemed to be more rigid due to their binding to LZY3016.

The energy decomposition demonstrated that the residue Lys-112 has a moderate electrostatic contribution, with the ΔE_{ele} of < -4.5 kcal mol^{-1} (Fig. 4A), because the amino acid Lys-112 was oriented to the benzoquinone group of the LZY3016, forming the cation-π interaction (Fig. 4B–D).[25] In addition, the residue Asn-106 has an excellent van der Waals contribution with the ΔE_{vdw} value less than -3.5 kcal mol^{-1} (Fig. 4A) due to the close-range between Asn-106 and LZY3016 (Fig. 4B–D). Except for the amino acid Asn-106, most of energy decomposition interactions were manifested as *van der Waals* interactions (Fig. 4A), mainly through hydrophobic interactions binding to LZY3016, such as Ala-55, Ile-96, Met-98, Leu-107 and Phe-138. Besides, the total binding free energy of Hsp90-LZY3016 complex was calculated based on the MMGBSA method, and

Table 4 The inhibitory effect of LZY3016 on MDA-MB-231 xenografts in nude mice

Compd	TGI (%)	T/C (%)
LZY3016	60.5	38.3
17-AAG	53.9	43.5

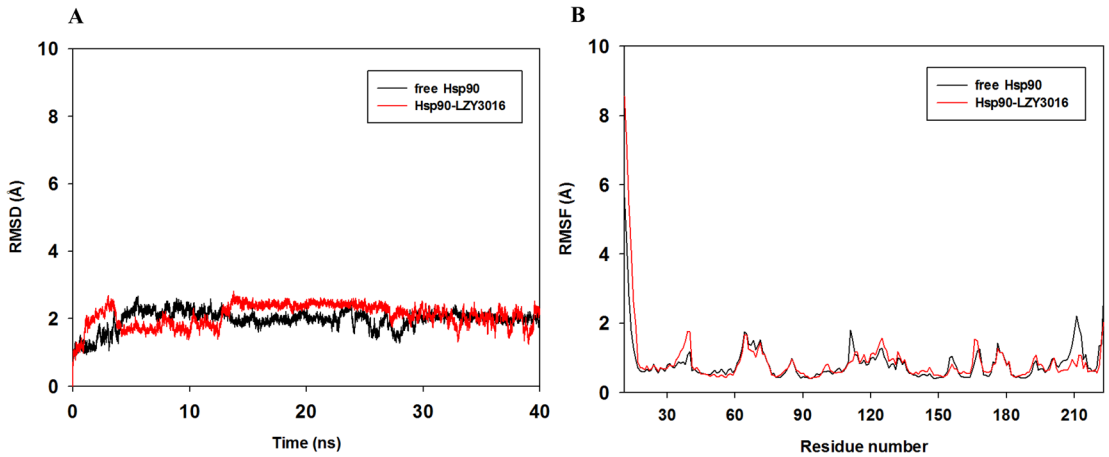

Fig. 3 The root-mean-square deviations (RMSDs) (in ångstrom) of all the atoms of free Hsp90 and Hsp90-LZY3016 complex during the 40 ns simulation (A). RMSF of residues of the whole protein in free Hsp90 and Hsp90-LZY3016 complex during the 40 ns simulation (B).

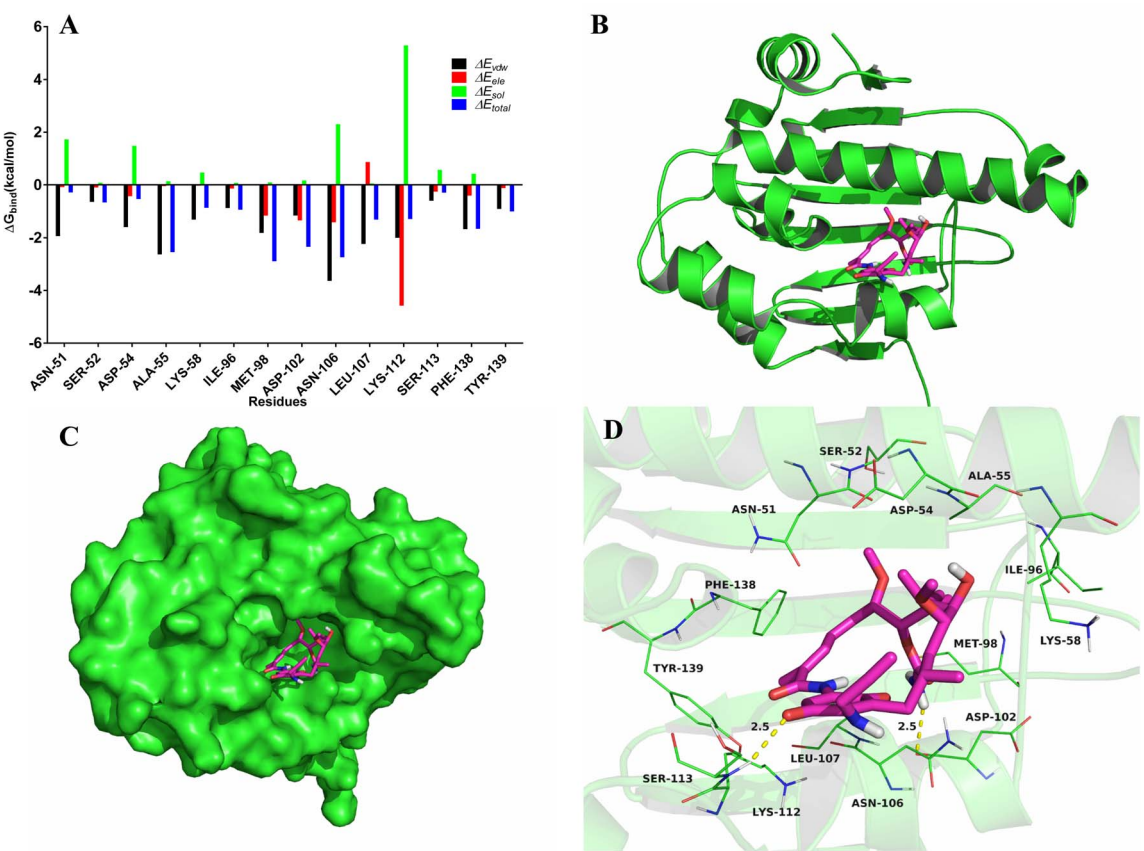

Fig. 4 Decomposition of the binding energy on a per-residue basis in the Hsp90-LZY3016 complex (A). The predicted binding mode of LZY3016 in Hsp90 binding pocket obtained from MD simulation (B–D).

the estimated ΔG_{bind} of LZY3016 was −43.1 kcal mol^{-1}, suggesting that LZY3016 can strongly bind to Hsp90.

4. Conclusions

In summary, a novel geldanamycin derivative LZY3016 was synthesized, which demonstrated potent anti-proliferation activity against MDA-MB-231 cell line, with an IC_{50} value of 0.06 μM. Hepatotoxicity evaluation test showed that the AST and ALT levels of LZY3016-treated group were both lower than those in GA-treated group. In addition, compared to 17-AAG, LZY3016 displayed more potent antitumor activity in the MDA-MB-231 xenograft model. The molecular modeling study revealed the theoretical binding model between LZY3016 and Hsp90 at

molecular level. All in all, LZY3016 has emerged as a potential hit for further design and development of novel Hsp90 inhibitors.

Conflicts of interest

We declare that we have no conflict of interest.

Acknowledgements

This work was supported by the National Natural Science Foundation of China (No. 81502921), and Shandong Provincial Natural Science Foundation (ZR2020MH399).

Notes and references

1 C. DeBoer, P. A. Meulman, R. J. Wnuk and D. H. Peterson, *J. Antibiot.*, 1970, **23**, 442–447.
2 C. E. Stebbins, A. A. Russo, C. Schneider, N. Rosen, F. U. Hartl and N. P. Pavletich, *Cell*, 1997, **89**, 239–250.
3 C. Moser, S. A. Lang and O. Stoeltzing, *Anticancer Res.*, 2009, **29**, 2031–2042.
4 J. G. Supko, R. L. Hickman, M. R. Grever and L. Malspeis, *Cancer Chemother. Pharmacol.*, 1995, **36**, 305–315.
5 E. A. Ronnen, G. V. Kondagunta, N. Ishill, S. M. Sweeney, J. K. DeLuca, L. Schwartz, et al., *Invest. New Drugs*, 2006, **24**, 543–546.
6 E. R. Glaze, A. L. Lambert, A. C. Smith, J. G. Page, W. D. Johnson, D. L. McCormick, et al., *Cancer Chemother. Pharmacol.*, 2005, **56**, 637–647.
7 H. Behrsing, K. Amin, C. Ip, L. Jimenez and C. Tyson, *Toxicol. In Vitro*, 2005, **19**, 1079–1088.
8 Z. Li, L. Jia, J. Wang, X. Wu, G. Shi, C. Lu, et al., *Chem. Biol. Drug Des.*, 2015, **85**, 181–188.
9 Z. Li, L. Jia, J. Wang, X. Wu, H. Hao, Y. Wu, et al., *Eur. J. Med. Chem.*, 2014, **87**, 346–363.
10 Z. Li, L. Jia, J. Wang, X. Wu, H. Hao, H. Xu, et al., *Eur. J. Med. Chem.*, 2014, **85**, 359–370.
11 Z. Li, L. Jia, H. Xu, C. Lu and Y. Shen, *Med. Chem.*, 2015, **11**, 482–488.
12 Z. Li, L. Jia, H. Tang, Y. Shen and C. Shen, *RSC Adv.*, 2019, **9**, 42509–42515.
13 Y. Zhang, H. Fang, J. Feng, Y. Jia, X. Wang and W. Xu, *J. Med. Chem.*, 2011, **54**, 5532–5539.
14 O. Trott and A. J. Olson, *J. Comput. Chem.*, 2010, **31**, 455–461.
15 H. M. Berman, J. Westbrook, Z. Feng, G. Gilliland, T. N. Bhat, H. Weissig, et al., *Nucleic Acids Res.*, 2000, **28**, 235–242.
16 S. K. Burley, C. Bhikadiya, C. Bi, S. Bittrich, H. Chao, L. Chen, et al., *Nucleic Acids Res.*, 2023, **51**, D488–D508.
17 M. F. Sanner, *J. Mol. Graphics Modell.*, 1999, **17**, 57–61.
18 G. M. Morris, R. Huey, W. Lindstrom, M. F. Sanner, R. K. Belew, D. S. Goodsell, et al., *J. Comput. Chem.*, 2009, **30**, 2785–2791.
19 L. C. Pierce, R. Salomon-Ferrer, C. A. F. de Oliveira, J. A. McCammon and R. C. Walker, *J. Chem. Theory Comput.*, 2012, **8**, 2997–3002.
20 A. W. Götz, M. J. Williamson, D. Xu, D. Poole, S. Le Grand and R. C. Walker, *J. Chem. Theory Comput.*, 2012, **8**, 1542–1555.
21 R. Salomon-Ferrer, A. W. Götz, D. Poole, S. Le Grand and R. C. Walker, *J. Chem. Theory Comput.*, 2013, **9**, 3878–3888.
22 A. A. Elfiky, H. A. Mahran, I. M. Ibrahim, M. N. Ibrahim and W. M. Elshemey, *RSC Adv.*, 2022, **12**, 2741–2750.
23 Y. Kasuya, Z. Lu, P. Kopeckova and J. Kopecek, *Bioorg. Med. Chem. Lett.*, 2001, **11**, 2089–2091.
24 F. Wuest, V. Bouvet, B. Mai and P. LaPointe, *Org. Biomol. Chem.*, 2012, **10**, 6724–6731.
25 J. C. Ma and D. A. Dougherty, *Chem. Rev.*, 1997, **97**, 1303–1324.